J Mol Model (2013) 19:2329–2334
DOI 10.1007/s00894-013-1773-4

ORIGINAL PAPER

Comparative studies for evaluation of CO_2 fixation in the cavity of the Rubisco enzyme using QM, QM/MM and linear-scaling DFT methods

Morad M. El-Hendawy · Niall J. English · Damian A. Mooney

Received: 22 August 2012 / Accepted: 14 January 2013 / Published online: 8 February 2013

Abstract We evaluate the minimum energy configuration (MM) and binding free energy (QM/MM and QM) of CO_2 to Rubisco, of fundamental importance to the carboxylation step of the reaction. Two structural motifs have been used to achieve this goal, one of which starts from the initial X-ray Protein Data Bank structure of Rubisco's active centre (671 atoms), and the other is a simplified, smaller model (77 atoms) which has been used most successfully, thus far, for study. The small model is subjected to quantum chemical density functional theory (DFT) studies, both *in vacuo* and using implicit solvation. The effects of the protein environment are also included by means of a hybrid quantum mechanical/molecular mechanical (QM/MM) approach, using PM6/AMBER and B3LYP/AMBER schemes. Finally, linear-scaling DFT methods have also been applied to evaluate energetic features of the large motif, and the result obtained for the binding free energy of the CO_2 underlines the importance of the accurate modelling of the surrounding protein milieu using a full DFT description.

Keywords Carboxylation step · Linear-scaling DFT · PM6 · QM/MM · Rubisco

M. M. El-Hendawy · N. J. English (✉) · D. A. Mooney (✉)
The SFI Strategic Research Cluster in Solar Energy Conversion,
University College Dublin, Belfield,
Dublin 4, Ireland
e-mail: niall.english@ucd.ie
e-mail: damian.mooney@ucd.ie

N. J. English · D. A. Mooney
The Centre for Synthesis and Chemical Biology,
School of Chemical and Bioprocess Engineering,
University College Dublin, Belfield,
Dublin 4, Ireland

Introduction

Ribulose-1,5 bisphosphate carboxylase oxygenase (RuBisCO, or Rubisco) is an enzyme which catalyses the carboxylation of ribulose 1,5-bisphosphate, RuBP, to yield two molecules of D-3-phosphoglyceric acid (PGA) [1]. It remains one of the most important and intriguing enzymes known to man, representing the key plant enzyme involved in the first (and rate-limiting) step of the fixation of atmospheric CO_2 (Calvin cycle). It is also the world's most abundant enzyme, accounting for up to 30–50% of the soluble leaf protein in C_4 and C_3 plants, respectively; suggesting that there is between 5 and 10 kg of Rubisco for every person on earth [2] converting on the order of 10^{11} CO_2 per annum into organic material [3]. However, its abundance has been seen as direct result of its perceived inefficiency [1, 4–6]. This inefficiency is marked by two main observations: 1) low catalytic rate of carboxylation per active site (k_{cat}) (between 3 and 10 s^{-1}) and 2) the competition between the dual functions of the enzyme in catalysing carboxylation (reacting with CO_2) relative to oxygenation (reacting with O_2), i.e. its specificity factor (τ) (ranging from 10 (purple photosynthetic bacteria) to 80 (C3 and C4 plants)) [7], where $\tau = V_{CO_2}K_{O_2}/V_{O_2}K_{CO_2}$ (the V_x corresponds to the maximum reaction velocity and the K_x correspond to the Michaelis constants, where x is either CO_2 or O_2) [8].

Its unique place in catalysing the conversion of large amounts of inert inorganic carbon, CO_2, into organic carbon has given it even greater significance in recent times; if harnessed appropriately, it provides a tantalising win-win proposition in both supplying a sink for anthropogenic CO_2 and yielding useful, accessible organic material which could not only be used to increase food production but could also supplement the raw materials and fuel supplied by traditional, fossil-based hydrocarbons [6, 9, 10].

Unfortunately, due to the complexity of the enzyme, it is still largely unknown what the rate-limiting step in the process Calvin cycle is; whether it is one of the steps in its actual reaction with RuBP (to yield PGA) or is it the diffusion mechanism of substrate/product through the protein. A significant body of literature has, therefore, built up over the past 10 to 20 years in trying to understand the structure and function of Rubisco with the expressed aim of either applying genetic engineering in improving its efficiency in fixing CO_2 for food, and/or biofuel production [1, 3, 5, 7, 11–16], or in seeking inspiration from it in developing synthetic analogues capable of yielding small molecular weight organic feedstock or fuels.

In any event, the study and elucidation of structural features concerning the molecular mechanism of carboxylation in Rubisco remains an important field of research, in view of the goal of achieving a deeper understanding of this process per se, but also rooted in the notion that such insights could yield the ultimate goal of synthesising alternative Rubisco-inspired organic and inorganic analogues. To this end, molecular modelling can offer many insights into deepening our understanding of the key interactions, and structural and reactive properties in the Rubisco active site. In particular, Kannappan and Gready [15] have made impressive progress in this field with their seminal work on molecular modelling of various reactive pathways in Rubisco. However, the increase in computer power in the past few decades, and, crucially, algorithmic advances in linear-scaling DFT [17], permits the accurate study of larger system sizes to thousands of atoms [18, 19], and the modelling of entire proteins [20, 21]. This allows for the inclusion of the protein matrix well beyond the active site, which QM and QM/MM neglect by necessity, due to its computationally prohibitive nature.

The goal of this study is to evaluate the Gibbs free energy of CO_2 fixation in Rubisco, using quantum mechanical (QM), QM/MM and linear-scaling DFT approaches, in order to assess the importance of inclusion of the surrounding protein milieu for the accurate determination of fixation thermodynamics. We have also conducted MM using different force-field models to calculate, for qualitative purposes, the minimum energy configuration for bound CO_2. To accomplish this, two structural motifs have been used, one of which starts from the initial X-ray Protein Data Bank structure of Rubisco's active centre (with 671 atoms) for MM, QM/MM and linear-scaling DFT, and the other is a simplified smaller model comprising 77 atoms for QM studies. In all cases, continuum solvation and *in vacuo* calculations are carried out to test explicitly solvation effects.

Methods

The 1.6 Å-resolution X-ray structure of an activated complex of Rubisco from spinach (i.e. *Spinacia oleracea*) was obtained from the Research Collaboratory for Structural Bioinformatics Data Bank (www.pdb.org) [22], with PDB entry code 8RUC [23]. The active site of the subunit L (residues 113 to 463) was taken from the whole structure, including the coordinated magnesium ion. This was achieved by taking all residues in all chains within a *circa* 24 Å radius of the Mg^{2+} ion—a rather expansive view of the active site. Missing residues were then added using MODELLER 9v8 [24], while hydrogen and missing atoms were added using the internal coordinates of the AMBER [25] topology files, assuming a pH of 7.5 for protonation states, resulting in 5458 atoms. Continuum solvation model (PCM) was to be used for subsequent estimates of solvation effects upon CO_2 fixation energetics. We used an empirical dielectric constant of 4, as there is consensus in the literature that this value gives a generally good agreement with experimental results and accounts for the average effect of both the protein and buried water molecules.

Molecular mechanics (MM) calculations were carried out in conjunction with the AMBER 99 parameter set [26] which includes the much improved potential parameters for Mg^{2+} as proposed by Aqvist [27]. We have also tested three different potential models for CO_2 including that contained with Amber99, as well as the EPM parameters developed by Harris and Yung [28] and the more recent model developed by Velanga et al. [29]. A summary of the corresponding force-field parameters are shown in Table 1. For MM calculations, we performed energy minimisation (0 K MM) in the gas phase, using the BORN solvation approximation as well as using explicit (TIP3P) water molecules [30]. In the latter case, we solvated the 671 protein fragment in a water-droplet of a diameter ~ 50 Å, such that the peripheral atoms of the protein were at least 6 Å from the edge of the drop. The outermost water molecules were restrained using a weak harmonic potential.

For the active site, in the carbamylated lysine (Lys 201), the parameters developed by Pang were employed [31]. A cut-off distance of 25 Å was applied to non-bonded interactions, to allow for detailed and converged studies of the CO_2-protein interaction energy as a function of protein milieu: the CO_2 molecule was placed in its binding position in the active site following energy minimisation and the interaction energy was found to converge to within 10% of that for the whole 5548-atom protein system in a smaller

Table 1 Lennard-Jones and charge force-field parameters for CO_2 used in this work

	σ_{C-C}/Å	σ_{O-O}/Å	ε_{C-C}/k	ε_{O-O}/k	q_C	q_O
AMBER 99 [26, 27]	3.400	2.960	43.300	105.73	0.974	−0.487
Harris-Yung [28]	2.757	3.033	28.129	80.507	0.652	−0.326
VVA [29]	3.595	2.975	76.765	56.414	0.652	−0.326

671-atom protein system by systematic removal of residues in onion-like 'shells' further from the CO_2. This was found to be a suitable system size for subsequent MM, QM/MM and linear-scaling DFT calculations. We employ a 25 Å cut-off for MM calculations as this was sufficient to include the entire 671 atom fragment (representing our model of Rubisco) when calculating the energies of the CO_2 molecule.

Several trials have been carried out to create a simplified fragment model that can realistically represent the active site of Rubisco and produce reliable energetics using QM calculations [15, 32–37]. Kannappan and Gready examined and assessed the validity of all suggested models [15]. They concluded that a 77-atom fragment model is sufficiently large as a reasonable representation of the active site, starting from enediolate intermediate, to study the CO_2 and O_2 fixation processes; we employed this fragment (designated FM20 in their paper [15]) in this study (cf. Fig. 1), as a representative system for viable QM calculations. It contains four-carbon (4C) for substrate, an $-OPO(OH)_2$ group attached to C1 (the charge on which has been neutralised via two protons to prevent artificial energetics for the species). Two CH_3COO^- ions were placed in lieu of ASP203 and GLU204 residues, and $CH_3NH_3^+$ ions were used to replace LYS175 and LYS177. One water molecule was added to complete the octahedral motif (cf. Fig. 1). HIS294 and LYS334 were modelled explicitly by an imidazole ring and NH_4^+ ions, respectively. The small and large systems are depicted in Fig. 2.

QM and QM/MM calculations were performed using density functional theory (DFT) with the B3LYP/6–31+g

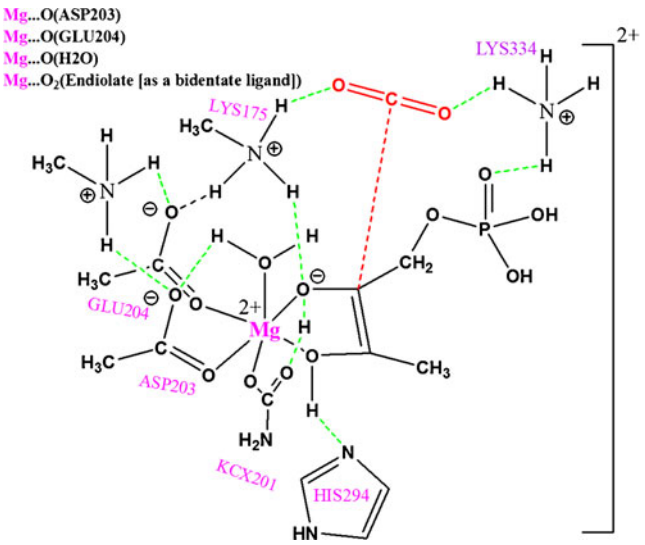

Fig. 1 Fragment model representing the active centre of Rubisco. The structure corresponds to the coordination sphere of Mg^{2+} centre with enediolate-bound CO_2. The fragment involves a hydrogen bond network, represented by green lines. The Mg…O bonds of the first coordination sphere are displayed in the top left

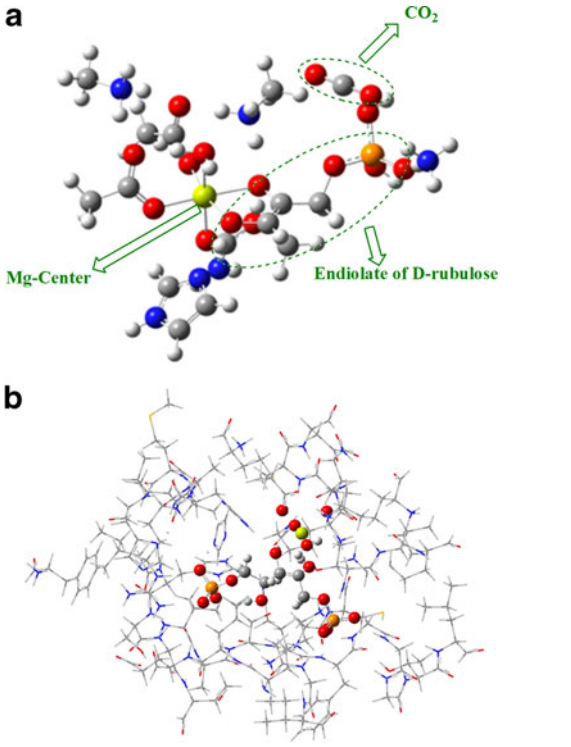

Fig. 2 Representation of the Rubisco active site, with **a** 77 atoms **b** 671 atoms, for respective use in QM (case a) and MM, QM/MM and linear-scaling DFT (case b)

(p,d) functional [38, 39] as implemented in Gaussian 09 suite [40], along with further MM calculations on geometry-optimised structures, with CO_2 placed adjacent the Mg ion (cf. Fig. 1). The functionals employed are those most commonly utilised in the techniques employed. Therefore, this work does not represent a systematic overview of these techniques, per se, but rather an attempt to present the typical range to be expected for the different levels of approximation. Frequency calculations were performed at the same level of optimisation to obtain zero-point energies (ZPE) and to ensure the absence of any negative eigenvalues. The energies so obtained were corrected for zero-point energy at 298 K. QM/MM calculations were carried out using the ONIOM [41, 42] approach on the 671-atom system, with the inner 77 atoms of the QM region serving as the inner layer, treated using PM6 [43] or B3LYP/6-31G(d,p) [38, 39, 44] approach and the outer region using AMBER. As well as performing QM (77-atom system) and MM, QM/MM calculations *in vacuo* (671-atom system), the PCM solvation model [45] was also used for water, as implemented in Gaussian 09, in geometry optimisation of the QM, MM and QM/MM systems, to allow for the assessment of solvation effects on fixation free energies. Here, electronic embedding scheme has been used which plays the fundamental role in the non-bonded interactions between the QM and MM regions.

Linear-scaling DFT was applied to optimise CO_2 binding to the 671-atoms system in the ONETEP package, which exploits "near-sightedness" of the density matrix [17]. The Perdew-Burke-Ernzerhof (PBE) functional [46] of the generalised gradient approximation (GGA) was used [47]. Non-orthogonal generalised Wannier functions (NGWFs), localised in real space, were used to represent the density matrix, with truncation radii of 4.6 Å. For NGWFs, a 1s configuration was used for H, a 2s2p for C, N and O, and a 3s configuration for Mg. The NGWFs were expanded in a basis of periodic cardinal sine (psinc) functions [48] with a kinetic energy cut-off of 750 eV. Core electrons were treated using norm-conserving pseudopotentials. Van der Waals interactions were included in the DFT energy by damped London potentials optimised for the PBE functional [49]. For all but MM calculations, the CO_2 binding free energy was evaluated *in vacuo* [50] on the geometry optimised structure [51], and in continuum solvation water using a Poisson Boltzmann surface area (PBSA) approach [52].

Table 3 Gibbs free energies of CO_2 fixation using various methods. Also shown is the angle taken by the O=C=O species (within the newly formed $-COO^-$ group) created by the reaction between CO_2 with the Enediolate form of RuBP. The average angle for this group from the experimental structure, 8RUC, is 118.2° (± 1.3°). Finally, the total CPU hours for each calculation is shown (=total time in hours × number of CPUs). All calculations were based on structures with 671 atoms, except full QM which was based on a structure with 77 atoms

Model (energies in kcal mol^{-1}; angles in degrees)	ΔG^{gas}	$\Delta G^{solv.}$	∠O-C-O	CPU hrs.
QM/MM: PM6:AMBER	−12.2	−12.9	113.3	~ 36
QM/MM: B3LYP/6-31+g(d,p): AMBER	−8.2	−9.6	125.5	~ 120
QM: B3LYP/6-31+g(d,p)	−6.8	−8.1	127.7	~ 168
L.S.-DFT: PBE/dispersion	−4.6	−5.1	118.8	~ 240

LS DFT timing is longer than full QM (Table 3). It seems to be contradictory. The level of calculations is slightly different, but I should not think that DFT, especially with empiric dispersion, such as that by Grimme (known as DFT-D) should be a lower level calculation compared to what the authors used with LS DFT. Some discussion of this should be added

Results and discussion

The first series of calculations were conducted using MM, as already discussed. The results of these calculations are shown in Table 2. While it is not suggested that these results can be compared with those presented in Table 3 (which are for structures in a reacted/bound state), it is certainly useful from a qualitative point of view to compare the results achieved using different models for CO_2, but also the effect of using different solvation models. Care, of course, should also be taken when comparing the results of minimisations which are not definitively global. Despite this, it is clear that the treatment of water has a very significant effect on energies as well as geometry. On the whole it appears to reduce the overall binding energy as well as stabilise the CO2 in a more proximate and strained conformation. The force-field of Velanga et al. seems to buck the trend regarding the d_{C-Mg} distance observed.

The binding free energies of CO_2 for QM/MM and QM calculations are provided in Table 3 for *in vacuo* and in continuum-solvent water. As one would expect, the inclusion of continuum solvation tends to render the binding free energy more negative. Although not available, one would expect that the results from MM (AMBER) are rather different (lower) to those of QM-type methods, indicating over-binding to some extent. Indeed, Fox et al. [50] have observed that binding energies are often lower (i.e. more negative) for AMBER than the corresponding full-scale

Table 2 Comparison of calculated MM energies (0 K total energy) for different models of CO_2 in the gas phase, BORN-solvation and explicit water descriptions for the system under investigation. In the case of explicit waters, the entire system was solvated into a water droplet where the outer layer of water molecules was constrained using an harmonic potential. In this later case, 1645 water molecules were included. All energies are in kcal mol^{-1}. HY refers to minimisations utilising the Harris-Yung potential [28] for CO_2. VVA refers to minimisations utilising the Velanga et al. potential for CO_2 [29]. ∠O-C-O refers to the angle subtended by CO_2. d_{C-Mg} refers to the separation (in Å) between the carbon atom of CO_2 and the Mg^{2+} ion

Model	E_{MM}	E_{vdW}	E_{elec}	E_{solv}	∠O-C-O°	d_{C-Mg} [Å]
MM: Amber 99 (Gas Phase)	−14.185	−8.492	−5.693	–	176.8	5.83
MM: Amber 99 (BORN)	−6.573	−6.924	−6.363	6.715	178.0	5.68
MM: Amber 99 (Explicit)	−11.221	−9.666	−1.556	–	175.1	4.77
MM: Amber 99/HY (Gas Phase)	−8.041	−6.289	−1.752		179.3	4.77
MM: Amber 99/HY (BORN)	−5.675	−6.130	−2.246	2.702	178.4	6.07
MM: Amber 99/HY (explicit)	−9.779	−7.233	−2.545	–	177.9	4.69
MM: Amber 99/VVA (Gas Phase)	−10.734	−8.489	−2.245		178.3	5.03
MM: Amber 99/VVA (BORN)	−7.776	−7.649	−2.259	2.133	179.6	7.83
MM: Amber 99/VVA (explicit)	−10.598	−7.885	−2.714	–	176.5	6.97

DFT results on identical systems. As fixed-charge MM forcefields, such as AMBER, neglect polarisation in their parameterisation, this may serve to rationalise why over-binding is sometimes observed when using MM, with energetic stabilisation over-emphasised. A better approximation in the classical domain would be to employ an increasingly sophisticated hierarchy of classical approximations including an appropriately adapted shell model and a suitable polarisable force field. QM/MM results are intermediate in binding energies vis-à-vis QM and linear-scaling DFT, at −12.2 to −12.9 kcal mol^{-1}; again, the energetic stabilisation afforded by a lack of polarisation may serve to explain this. However, it is likely that the artifact of the QM/MM boundary affects results substantially. More convincing binding energies, especially when compared to metallo-proteins of comparable size [50] are the results from pure QM and linear-scaling DFT. The QM result of −6.8 to −8.1 kcal mol^{-1} appears to be affected to some extent (almost 20%) by solvation, as one would expect from such a necessarily small system of 77 atoms. This size artifact is very problematic, given that the protein environment surrounding the CO_2 would be expected to play a substantial role in modulating the energetic and mechanics of interaction with the complex. In this respect, the linear-scaling DFT result of −4.6 to −5.1 kcal mol^{-1} is most appealing and convincing, with a solvation correction of approximately 10% vis-à-vis the gas-phase result. A very useful discussion on the influence of solvation on binding energies is provided by Murata et al. [53].

Also shown in this table is the angle subtended by the O-C-O ($-COO^-$) species created by the reaction of CO_2 with the Enediolate form of RuBP, namely 2-carboxy-3-keto-D-arabinitol 1,5-bisphosphate (CKABP). This very simple structural determinant provides some evidence as to the utility of each of the techniques used in predicting/supporting experimental observables. As can be seen from this table, LS-DFT replicates experiment remarkably well, yielding a value of 118.8°, while experiment yields a value of 118.2±1.3°.

Conclusions

Preliminary MM energy minimisation calculations on CO_2 at the active site of Rubisco reveal both the effect of different CO_2 force-field parameters, as well as the importance of water in stabilising CO_2 near the active site. It has also been found that linear-scaling DFT leads to important corrections in a more accurate and satisfactory estimate of CO_2 binding free energy to Rubisco, in conjunction with PCM correction, relative to the QM/MM approach and also smaller-scale QM estimates. Given the importance of Rubisco and the ultimate goal of using computational design to lead in the predictive *in silico* design of biomimetic carbon capture materials, the accurate, full-system treatment of evaluation of thermodynamic parameters is vital for assessing potential for CO_2 fixation. This study confirms this. It is also to be expected that linear-scaling DFT will find many other applications in biology, chemistry, chemical physics and materials science.

Acknowledgments The authors acknowledge useful conversations with Jacek Dziedzic, Chris-Kriton Skylaris, Peter Haynes, Daniel Cole and Nicholas Hine. The research was funded primarily by the Science Foundation Ireland (SFI)-funded Solar Energy Conversion (SEC) research cluster [Grant No. 07/SRC/B1160], with input from SFI Research Frontiers Programme 10/RFP/MTR2868. We thank SFI for the provision of funds for high-performance computing facilities and the Irish Centre for High-End Computing (ICHEC) for computational resources. The authors acknowledge the support of industry partners to the SEC cluster: SolarPrint, Celtic Catalysts, Glantreo, Mainstream Renewable Power, Kingspan and SSE Renewables.

References

1. Berg JM, Tymoczko JL, Stryer L (2007) Biochemistry, 6th edn. W. H. Freeman, New York
2. Griffiths H (2006) Nature 441:940–941
3. Portis AR, Parry MAJ (2007) Photosynth Res 94:121–143
4. Spreitzer RJ, Salvucci ME (2002) Annu Rev Plant Biol 53:449–475
5. Sage RF, Way DA, Kubien DS (2008) J Exp Bot 59:1581–1595
6. Parry MAJ, Andralojc PJ, Mitchell RAC, Madgwick PJ, Keys AJ (2003) J Exp Bot 54:1321–1333
7. Taiz L, Zeiger E (2010) Plant physiology, 5th edn. Sinauer, Sunderland
8. Galmés J, Flexas J, Keys AJ, Cifre J, Mitchell RAC, Madgwick PJ, Haslam RP, Medrano H, Parry MAJ (2005) Plant Cell Environ 28:571
9. Evans JR, Kaldenhoff R, Genty B, Terashima I (2009) J Exp Bot 60:2235–2248
10. Mott KA, Woodrow IE (2000) J Exp Bot 51:399–406
11. Ragauskas AJ, Williams CK, Davison BH, Britovsek G, Cairney J, Eckert CA, Frederick WJ, Hallett JP, Leak DJ, Liotta CL, Mielenz JR, Murphy R, Templer R, Tschaplinski T (2006) Science 311:484
12. Sage RF, Kubien DS (2007) Plant Cell Environ 30:1086
13. Evans JR, Kaldenhoff R, Genty B, Terashima I (2009) J Exp Bot 60:2235
14. Mott KA, Woodrow IE (2000) J Exp Bot 51:399
15. Kannappan B, Gready JE (2008) J Am Chem Soc 130:15063
16. King WA, Gready JE, Andrews TJ (1998) Biochemistry-Us 37:15414
17. Skylaris CK, Haynes PD, Mostofi AA, Payne MC (2005) J Chem Phys 122
18. Hine NDM, Haynes PD, Mostofi AA, Skylaris CK, Payne MC (2009) Comput Phys Commun 180:1041
19. Gordon MS, Fedorov DG, Pruitt SR, Slipchenko LV (2012) Chem Rev 112:632
20. Cole DJ, Rajendra E, Roberts-Thomson M, Hardwick B, McKenzie GJ, Payne MC, Venkitaraman AR, Skylaris CK (2011) PLoS Comput Biol. doi:10.1371/journal.pcbi.1002096
21. Cole DJ, Skylaris CK, Rajendra E, Venkitaraman AR, Payne MC (2010) EPL. doi:10.1209/0295-5075/91/37004
22. Bernstein FC, Koetzle TF, Williams GJB, Meyer EF, Brice MD, Rodgers JR, Kennard O, Shimanouchi T, Tasumi M (1977) Eur J Biochem 80:319

23. Andersson I (1996) J Mol Biol 259:160–174
24. Marti-Renom MA, Stuart AC, Fiser A, Sanchez R, Melo F, Sali A (2000) Annu Rev Biophys Biomol 29:291–325
25. Cornell WD, Cieplak P, Bayly CI, Gould IR, Merz KM, Ferguson DM, Spellmeyer DC, Fox T, Caldwell JW, Kollman PA (1995) J Am Chem Soc 117:5179
26. Wang J, Cieplak P, Kollman PAJ (2000) Comput Chem 21:1049
27. Aaqvist J (1990) J Phys Chem 94:8021
28. Harris JG, Yung KH (1995) J Phys Chem 99:12021
29. Velanga S, Vedam V, Anderson BJ (2011) In 7th International Conference on Gas Hydrates (ICGH 2011), Proc: Edinburgh, Scotland, United Kingdom, 2011
30. Jorgensen WL, Chandrasekhar J, Madura JD, Impey RW, Klein MLJ (1983) Chem Phys 79:926
31. Pang YP (2001) Proteins 45:183–189
32. King WA, Gready JE, Andrews TJ (1998) Biochemistry-Us 37:15414–15422
33. Oliva M, Safont VS, Andres J, Tapia O (1999) J Phys Chem A 103:8725
34. Oliva M, Safont VS, Andres J, Tapia O (1999) J Phys Chem A 103:6009
35. Oliva M, Safont VS, Andres J, Tapia O (2001) Chem Phys Lett 340:391
36. Tapia O, Andres J, Safont VS (1995) J Mol Struct THEOCHEM 342:131–140
37. Zhang X, Bruice TC (2007) Biochemistry-Us 46:14838–14844
38. Becke AD (1993) J Chem Phys 98:5648–5652
39. Lee CT, Yang WT, Parr RG (1988) Phys Rev B 37:785–789
40. Gaussian 09, Revision A.1, Frisch MJ, Trucks GW, Schlegel HB, Scuseria GE, Robb MA, Cheeseman JR, Scalmani G, Barone V, Mennucci B, Petersson GA, Nakatsuji H, Caricato M, Li X, Hratchian HP, Izmaylov AF, Bloino J, Zheng G, Sonnenberg JL, Hada M, Ehara M, Toyota K, Fukuda R, Hasegawa J, Ishida M, Nakajima T, Honda Y, Kitao O, Nakai H, Vreven T, Montgomery Jr. JA, Peralta JE, Ogliaro F, Bearpark M, Heyd JJ, Brothers E, Kudin KN, Staroverov VN, Kobayashi R, Normand J, Raghavachari K, Rendell A, Burant JC, Iyengar SS, Tomasi J, Cossi M, Rega N, Millam JM, Klene M, Knox JE, Cross JB, Bakken V, Adamo C, Jaramillo J, Gomperts R, Stratmann RE, Yazyev O, Austin AJ, Cammi R, Pomelli C, Ochterski JW, Martin RL, Morokuma K, Zakrzewski VG, Voth GA, Salvador P, Dannenberg JJ, Dapprich S, Daniels AD, Farkas Ö, Foresman JB, Ortiz JV, Cioslowski J, Fox DJ (2009) Gaussian, Inc., Wallingford CT
41. Dapprich S, Komaromi I, Byun KS, Morokuma K, Frisch MJ (1999) J Mol Struct (THEOCHEM) 461:1
42. Vreven T, Morokuma K, Farkas O, Schlegel HB, Frisch MJ (2003) J Comput Chem 24:760–769
43. Stewart JJP (2007) J Mol Model 13:1173–1213
44. Stephens PJ, Devlin FJ, Chabalowski CF, Frisch MJ (1994) J Phys Chem-Us 98:11623–11627
45. Tomasi J, Mennucci B, Cammi R (2005) Chem Rev 105:2999–3093
46. Perdew JP, Burke K, Ernzerhof M (1996) Phys Rev Lett 77:3865–3868
47. Perdew JP, Wang Y (1992) Phys Rev B 45:13244–13249
48. Mostofi AA, Haynes PD, Skylaris CK, Payne MC (2003) J Chem Phys 119:8842–8848
49. Hill Q, Skylaris CK (2009) Public Relat Soc Am 465:669–683
50. Fox S, Wallnoefer HG, Fox T, Tautermann CS, Skylaris CK (2011) J Chem Theory Comput 7:1102–1108
51. Hine NDM, Robinson M, Haynes PD, Skylaris CK, Payne MC, Mostofi AA (2011) Phys Rev B 83
52. Dziedzic J, Helal HH, Skylaris CK, Mostofi AA, Payne MC (2011) Epl-Europhys Lett 95
53. Murata K, Fedorov DG, Nakanishi I, Kitaura K (2009) J Phys Chem B 113:809